Bone 122 (2019) 93–100

Contents lists available at ScienceDirect

Bone

journal homepage: www.elsevier.com/locate/bone

Full Length Article

Zscan10 suppresses osteoclast differentiation by regulating expression of *Haptoglobin*

Yuta Yanagihara[a,b], Kazuki Inoue[b,c], Noritaka Saeki[b,c], Yuichiro Sawada[c,d], Shuhei Yoshida[c], Jiwon Lee[e], Tadahiro Iimura[e,f], Yuuki Imai[a,b,c,*]

[a] Department of Pathophysiology, Graduate School of Medicine, Ehime University, Toon, Ehime, Japan
[b] Division of Laboratory Animal Research, Advanced Research Support Center, Ehime University, Toon, Ehime, Japan
[c] Division of Integrative Pathophysiology, Proteo-Science Center, Ehime University, Toon, Ehime, Japan
[d] Department of Urology, Graduate School of Medicine, Ehime University, Toon, Ehime, Japan
[e] Division of Bio-Imaging, Proteo-Science Center, Ehime University, Toon, Ehime, Japan
[f] Division of Analytical Bio-Medicine, Advanced Research Support Center, Ehime University, Toon, Ehime, Japan

ARTICLE INFO

Keywords:
Zscan10
Haptoglobin
Osteoclast differentiation
Osteoclasts
Transcription factors

ABSTRACT

Zinc finger and SCAN domain containing 10 (Zscan10) was identified as a novel transcription factor that is involved in osteoclast differentiation in our previous report. However, the biological functions of Zscan10 are not fully understood except its roles in the maintenance of genome stability and pluripotency of embryonic stem cells. Therefore, the purpose of this study was to clarify the function of Zscan10 in somatic cells, especially during osteoclast differentiation. First, *Zscan10* KO RAW264 (KO) cells were established by genome editing using CRISPR/Cas9 and single cell sorting. Then, control (Ctrl) and KO cells were differentiated into osteoclasts by RANKL stimulation. We observed that TRAP activity and the expression levels of differentiation marker genes, such as *Nfatc1*, were significantly increased and the expression of inhibitory factors, such as *Irf8*, was decreased in KO cells compared to Ctrl cells. These results suggest that Zscan10 might regulate transcription of the genes that negatively control osteoclastogenesis. To understand gene expression profiles controlled by Zscan10, RNA-seq was performed and stringent analyses identified the haptoglobin gene (*Hp*) as a possible target of Zscan10. In addition, ChIP against Zscan10 revealed that Zscan10 could interact with its binding motif located near the *Hp* gene locus as well as the transcription start site of *Hp*, suggesting that Zscan10 can directly regulate transcription of *Hp*. Finally, to examine the effects of Hp on osteoclastogenesis, KO cells were treated with recombinant Hp (rHp). rHp treatment suppressed TRAP activity of KO cells without affecting cell viability. Furthermore, it has been reported that *Hp* KO mice exhibit decreased bone mass and increased osteoclast number. Importantly, hemolytic disease patients exhibited decreased serum level of Hp as well as low bone mineral density. Taken together, this study suggests that Zscan10 negatively regulates osteoclast differentiation through transcription of *Hp*.

1. Introduction

Bone homeostasis is preserved by the balance between osteoclastic bone resorption and osteoblastic bone formation [1]. Loss of this balance causes bone metabolic diseases. Enhanced osteoclast differentiation causes osteoporosis, whereas suppression of osteoclastogenesis causes osteopetrosis [2]. Osteoclast differentiation occurs through various molecular pathways. In osteoclastogenesis, the critical regulatory pathway includes receptor activator of nuclear factor-kappa B (RANK) and RANK ligand (RANKL) [3]. This pathway promotes the activity of several transcription factors, including nuclear factor of activated T cells calcineurin-dependent 1 (Nfatc1) [4], nuclear factor-kappa B (NF-κB) [5], activator protein 1 (Ap1) [6] and cyclic adenosine monophosphate responsive-element-binding protein (Creb) [7]. Nfatc1 is a master transcription factor in osteoclast differentiation; it can induce the expression of osteoclastogenic genes including tartrate-resistant acid phosphatase (*Trap*) [8] and cathepsin K (*Ctsk*) [9]. Thus, the molecular mechanisms underlying osteoclast differentiation have been elucidated. However, epigenetic regulation in osteoclast differentiation is only poorly understood. Therefore, we have focused on epigenetic processes (chromatin remodeling) in osteoclast differentiation. Based on genome-wide analyses of open chromatin regions using DNase-seq,

* Corresponding author at: Department of Pathophysiology, Graduate School of Medicine, Ehime University, Shitsukawa, Toon, 791-0295, Ehime, Japan.
E-mail address: y-imai@m.ehime-u.ac.jp (Y. Imai).

https://doi.org/10.1016/j.bone.2019.02.011
Received 4 December 2018; Received in revised form 8 February 2019; Accepted 11 February 2019
Available online 13 February 2019
8756-3282/

sterol regulatory element-binding protein 2 (Srebp2), NF-E2-related factor 1 (Nrf1), activating transcription factor 1 (Atf1), and zinc finger and SCAN domain containing 10 (Zscan10) were identified as candidate novel transcription factors that may regulate osteoclast differentiation [10]. Evidence suggested that those candidate genes actually control osteoclast differentiation because Fatostatin, an inhibitor of Srebp2, inhibits RANKL-induced bone loss [11].

Zscan10 was identified as a novel transcription factor in osteoclast differentiation. However, little is known about this molecule. Zscan10, a member of the Zscan family, consists of 14 C2H2 zinc finger domains and an N-terminal SCAN domain [12]. Gene Ontology (GO) annotations related to this gene include DNA binding transcription factor activity and sequence-specific DNA binding, including the 5′-[GA]CGCNN GCG[CT]-3′ motif. > 3000 binding motifs of Zscan10 have been identified in the mouse genome [13]. Zscan10 is reportedly involved in maintaining the undifferentiated status and genome stability of ES cells by interacting with sex determining region Y-box 2 (Sox2) and octamer-binding transcription factor 4 (Oct4), well-known as pluripotent factors [12,14–17]. Zscan10 KO mice exhibit partial lethality after weaning as well as developmental abnormalities in the eye and a reduction in the number of ribs [18]. On the other hand, there is a report that Zscan10 is dispensable for mouse development [19], suggesting that the functions of Zscan10 are still controversial and remain elusive. Therefore, the purpose of this study was to clarify Zscan10 functions in somatic cells, especially osteoclast differentiation.

2. Materials and methods

2.1. Animals

C57BL6 female mice were purchased from CLEA Japan (Tokyo, Japan). Mice were housed in a specific pathogen-free facility under climate-controlled conditions at room temperature (22 ± 2 °C) with 50% humidity and a 12-h light/dark cycle. Mice were provided with water and standard diet (MF, Oriental Yeast Co. Ltd.) *ad libitum*. Animal experiments were approved by the Animal Experiment Committee of Ehime University and were performed in accordance with the Guidelines of Animal Experiments of Ehime University.

2.2. Cell culture and osteoclast differentiation

The murine macrophage-like cell line, RAW264, was obtained from RIKEN cell bank (Ibaraki, Japan). RAW264 cells were cultured in alpha-minimum Eagle's medium (α-MEM) (Life Technologies, Carlsbad, CA) supplemented with 10% CELLect fetal bovine serum (FBS) (MP Biomedicals, Santa Ana, CA, USA), 1% antibiotic-antimycotic solution (Life Technologies) and 1% minimum Eagle's medium nonessential amino acids (MEM-NEAA) (Life Technologies) at 37 °C in 5% CO_2 humidified air. RAW264 cells were seeded in plates and were treated with 150 ng/mL GST-RANKL (Oriental Yeast Co. Ltd. Tokyo, Japan) for 4–5 days. For recombinant human haptoglobin (rHp) (rPeptide, Watkinsville, GA, USA), cells were treated with 20 μg/mL of rHp 1 day before RANKL stimulation. FK506 (FUJIFILM Wako Pure Chemical Corporation, Osaka, Japan) was used as a calcineurin inhibitor and added to the culture medium (20 μg/mL) for 1 day after RANKL stimulation.

2.3. Isolation and culture of murine bone marrow macrophages

Murine bone marrow-derived macrophages (BMMs) were isolated from the tibias of C57BL6 female mice at 6 to 8 weeks of age. BMMs were cultured in α-MEM supplemented with 10% FBS, 1% antibiotic-antimycotic solution and treated with 100 ng/mL M-CSF (FUJIFILM Wako Pure Chemical Corporation, Osaka, Japan) and 150 ng/mL RANKL for an additional 4–5 days. BMMs were treated with 20 μg/mL of rHp 1 day before RANKL stimulation.

2.4. Establishment of Zscan10 knockout cells

Zscan10 KO RAW264 cells were established using the Guide-it™ CRISPR/Cas9 Systems (Takara Bio Inc., Kusatsu, Japan). *Zscan10*-specific gRNA (No.1: 5′-GGAGTTGTGAAAGATGCTGG-3′; PAM sequence, CGG: No.2: 5′-GCAGGAGTCCCTCACCTTTG-3′; PAM sequence: AGG) was designed using CHOPCHOP [20,21] and synthetic oligos were ligated into Guide-it-ZsGreen1 Vector. The plasmid vector was transfected into RAW264 cells with electroporation using a Neon® Transfection System (Life Technologies.) followed by single cell sorting of Zsgreen-positive cells with a FACSAria (Becton, Dickinson and Company, Franklin Lakes, NJ). KO cell colonies were verified by DNA sequence changes that induced frame shift and premature termination.

2.5. Cell proliferation assays

Cell proliferation was analyzed using a 3-(4,5-dimethylthiazol-2-yl)-2, 5-diphenyl tetrazolium bromide (MTT) cell count kit (Nacalai Tesque, Inc. Kyoto, Japan) and a Cell Proliferation ELISA Bromodeoxyuridine (BrdU) kit (F. Hoffmann-La Roche, Ltd. Basel, Switzerland). Cells were seeded at 1×10^4 per well into 96-well plates containing 100 μL culture medium per well. The BrdU assay was performed after serum starvation for 24 h to synchronize the cell cycle before analysis. Both assays were performed at 1 day after seeding.

2.6. TRAP activity assay

TRAP activity was assessed according to a previous report [22]. Briefly, osteoclasts were fixed with 10% neutralized formaldehyde at 4 or 5 days after RANKL stimulation and incubated in TRAP assay buffer (50 mM citrate buffer and 0.12 M sodium acetate, pH 4.6) containing 0.5 mg/mL *p*-nitrophenyl phosphate for 30 min at 37 °C. The reaction was stopped with 0.1 N NaOH, and the absorbance was measured at 405 nm.

2.7. Fluorescence staining

Osteoclasts were fixed with 4% paraformaldehyde phosphate buffer solution and washed with PBS, permeabilized in 0.2% Triton X-100/PBS and stained using Alexa Fluor™ 488 Phalloidin and DAPI (Life Technologies.).

2.8. Mature osteoclast occupying rate

Mature osteoclast occupying rate was determined as the proportion of area occupied by osteoclasts in the well and calculated from Phalloidin stained images using Image J [23].

2.9. Plasmid and transfection

Flag-tagged plasmid vector of *Zscan10* was constructed by subcloning *Zscan10* cDNA into pME18SII-FLAG-NT vector, kindly provided by Prof. Shigeki Higashiyama (Ehime University), using an In-Fusion® HD Cloning Kit (Takara Bio, Inc.). The plasmid was transfected into each cell by electroporation using a Neon® Transfection System (Life Technologies.).

2.10. Real-time RT-PCR (RT-qPCR)

Total RNA was extracted with ISOGEN (Nippon Gene CO., LTD. Tokyo, Japan) and reverse-transcribed into first-strand cDNA using a PrimeScript RT Master Mix (Takara Bio, Inc.) according to the manufacturer's instructions. RT-qPCR was performed with TB Green® Premix Ex Taq™ II (Takara Bio, Inc.) and a Thermal Cycler Dice Real-Time System (Takara Bio, Inc.). All sequences for primers used in this study are provided in Supplemental Table S1.

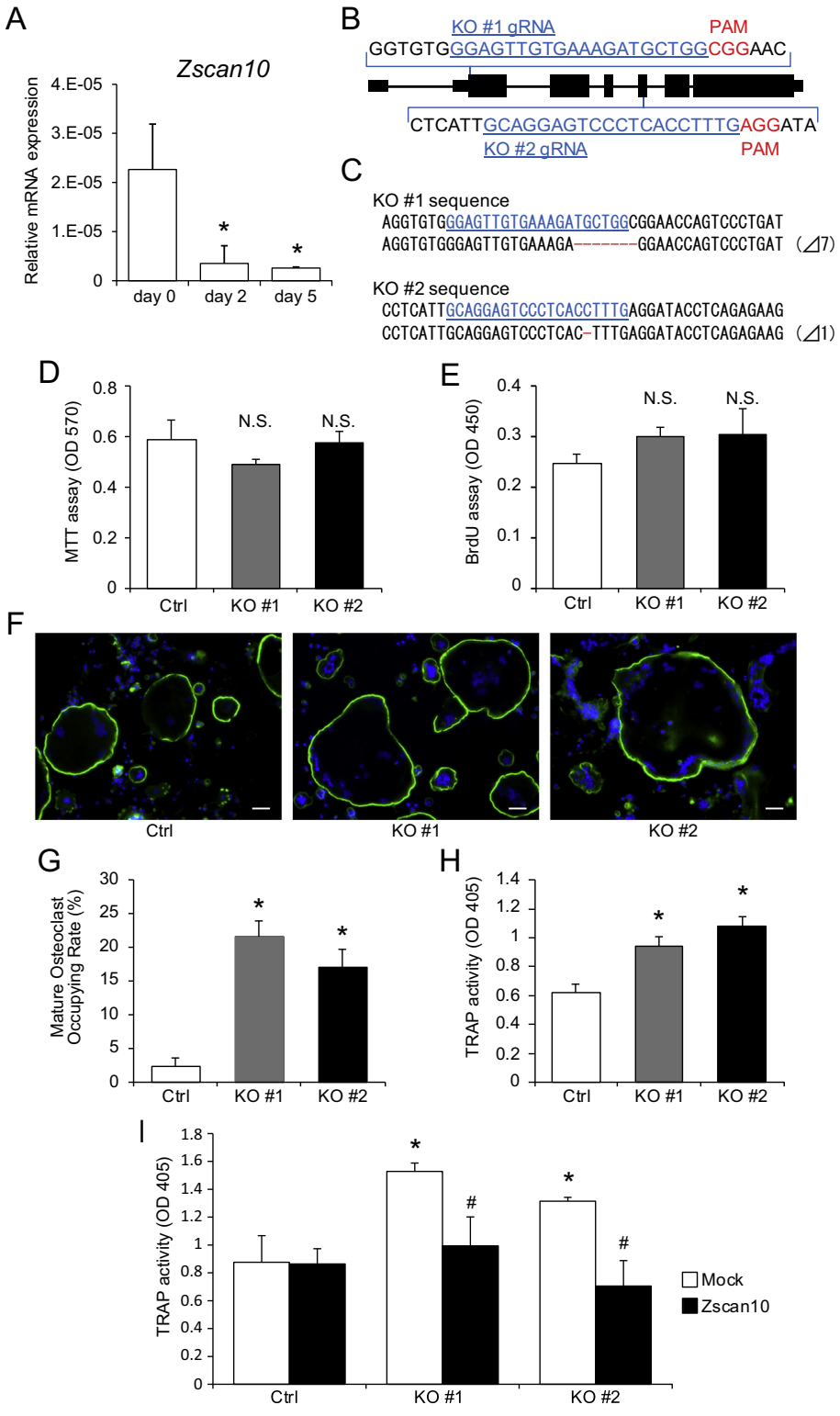

Fig. 1. Establishment of *Zscan10* KO RAW264 cells and its phenotype. (A) mRNA expression levels of *Zscan10* associated with osteoclast differentiation were determined by RT-qPCR. (B) Schematic panels of the targeting strategy to inactivate the *Zscan10* gene. (C) Direct sequencing results of KO cells. (D) Cell viability of Ctrl and KO cells assessed by MTT assay. (E) Assessment of Ctrl and KO cell proliferation by BrdU assay. (F) Fluorescence staining in Ctrl and KO cells; nuclear (blue) and actin (green). Bars indicate 50 μm. (G) Percentage of mature osteoclasts occupying arbitrary area. (H) TRAP activity of Ctrl and KO cells in mature osteoclasts. (I) TRAP activity of *Zscan10* overexpression in Ctrl and KO mature osteoclasts. Data represent means ± SD, n = 3. *p* values were analyzed using a one-way ANOVA followed by Tukey–Kramer method post hoc tests. Asterisk indicates $p < 0.05$ versus control. Sharp indicates $p < 0.05$ versus Mock. (For interpretation of the references to colour in this figure legend, the reader is referred to the web version of this article.)

2.11. RNA sequencing and bioinformatics analysis

The quality of the extracted RNA was assessed using a Bioanalyzer 2100 and RNA 6000 Nano Kit (Agilent Technologies, Inc. Santa Clara, CA) according to the manufacturer's instructions. An Illumina TruSeq Standard mRNA LT Sample Prep Kit (Illumina, Inc. San Diego, CA) was used for the library preparation. mRNA sequencing was performed using an Illumina MiSeq Reagent kit V3 150 cycle kit with 75 bp paired-end sequencing with a fragment size of ~260 bp, which were trimmed to 75 bp, and the obtained data were deposited in Gene Expression Omnibus (GSE121320). These data were mapped to mouse genome data mm10 using Tophat without trimming due to the quality of fastq data. Then, we performed gene expression analysis using two different methods, such as trimmed mean of M values (TMM) and fragments per kilobase of exon per million mapped reads (FPKM). Reads mapped from bam files were counted with featureCounts and then TMM was detected using exact test of edgeR package after normalizing count data with TCC package. FPKM was calculated using Cufflinks from mapping data.

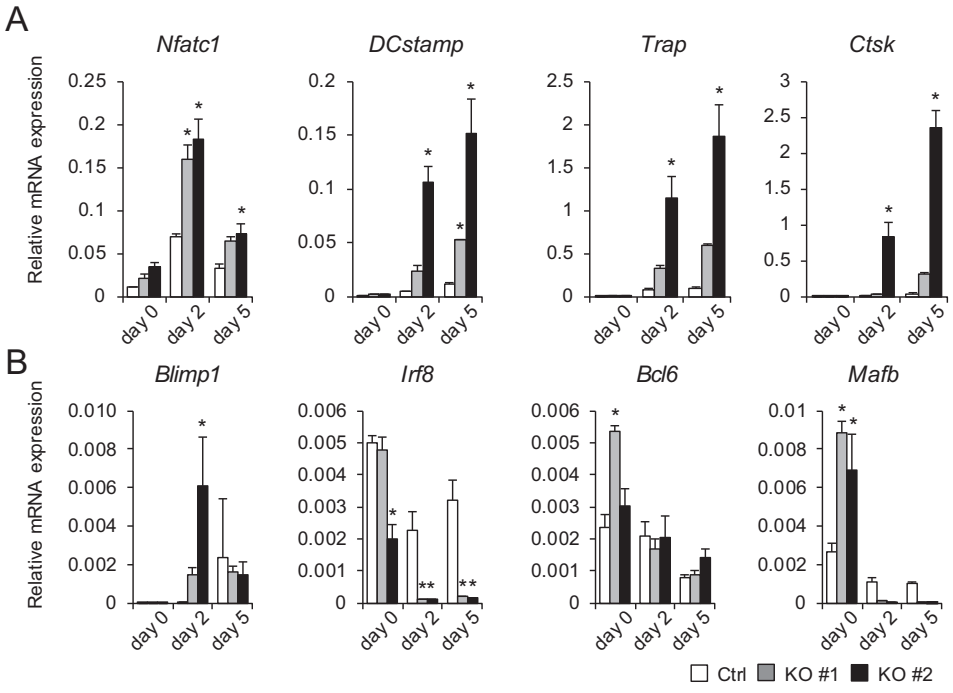

Fig. 2. mRNA expression levels of genes associated with osteoclast differentiation. (A) Relative mRNA expression of osteoclast differentiation markers (*Nfatc1*, *DCstamp*, *Trap*, *Ctsk*) during differentiation was measured by RT-qPCR. (B) Relative mRNA expression of osteoclast differentiation inhibitory factors (*Blimp1*, *Irf8*, *Bcl6*, *MafB*) during differentiation was measured by RT-qPCR. Data show means ± SD, n = 3. *p* values were analyzed using a one-way ANOVA followed by Tukey–Kramer method post hoc tests. Asterisk indicates $p < 0.05$ versus control.

Bioinformatic analyses and visualization were performed using bioinformatics resources such as DAVID [24,25], GALAXY [26] and IgV [27,28].

2.12. Chromatin immunoprecipitation (ChIP)-qPCR

ChIP was performed by constructing a Flag-tagged plasmid vector of *Zscan10* and overexpressing it in RAW264 cells. The protein-DNA complexes were obtained with an EpiXplore™ kit (Takara Bio, Inc.). The protein-DNA complexes were sonicated into fragments of approximately 200–2000 bp in length, and the fragmented chromatin samples were suspended in ChIP dilution buffer. Sheared chromatin was immunoprecipitated with 1 μg of anti-Flag antibodies (Sigma-Aldrich, St. Louis, MO) and Dynabeads protein G (Life Technologies). The eluted ChIPed protein-DNA complexes were treated with proteinase K and RNase A for 2 h at 55 °C, then DNA fragments were purified for quantitative PCR analysis. Specific primer sequences for the *Hp* gene locus were 5′-GCAAGTTGTCTCTGGCTCCT-3′ and 5′-CGTTGCCTTGGTTATG GTGT-3′ and the transcript start site (TSS) were 5′-CAGCCAGTGACCT TAGAGACG-3′ and 5′-CTCCGGCCGAGCCCTTTAT3′- As a negative control, primers 5′-CTGCAGTACTGTGGGGAGGT-3′ and 5′-CAAAGGC GGAGTTACCAGAG-3′ were designed for the locus without Zscan10 binding motif (Fig. 3F).

2.13. Statistical analysis

The data are presented as the mean ± standard deviation (SD). Statistical significance was determined using the SPSS (IBM, Armonk, NY, USA) software programs. The data were analyzed using a two-tailed Student's *t*-test or by a one-way analysis of variance (ANOVA) followed by Tukey–Kramer method post hoc tests. For all graphs, data are shown as means ± standard deviation (SD). Statistical significance was accepted when $p < 0.05$.

3. Results

3.1. Deficiency of Zscan10 accelerated osteoclast differentiation

In order to establish *Zscan10* knockout cells (KO), mRNA expression levels of *Zscan10* were examined along with osteoclast differentiation. We found that *Zscan10* mRNA expression levels were decreased after RANKL stimulation (Fig. 1A). Therefore, KO cells were established in murine macrophage-like RAW264 cells without RANKL treatment using a CRISPR/Cas9 system and single cell sorting. Two gRNAs were designed as shown in Fig. 1B. Sequencing showed that 7 bases and a single base deficiency accompanying a frame shift were present in 2 strains with clean single waveform (Fig. 1C and Supplemental Fig. S1A). In addition, TA-cloning of both cells suggested that these cells were homozygous mutant (Supplemental Fig. S1B). Also, premature termination was confirmed, i.e., a stop codon was contained in the middle of the amino acid sequence (Supplemental Fig. S2). These data confirmed that *Zscan10* KO strains in RAW264 cells were successfully established.

To examine the effects of *Zscan10* KO on RAW264 cells, we assessed cell viability and proliferation. We found that there were no differences between established KO cells and control (Ctrl) cells in MTT absorbance (Fig. 1D) and BrdU incorporation (Fig. 1E). Next, to test the effects on osteoclast differentiation, these cells were treated with RANKL. On the contrary to our expectation, both the number and size of osteoclasts differentiated from KO cells were larger than that observed with Ctrl cells (Fig. 1F). We calculated the proportion of the observed area occupied by osteoclasts and found that KO cells showed a significantly higher value (Fig. 1G). Also, KO cells displayed significantly higher TRAP activity when compared to Ctrl cells (Fig. 1H). Furthermore, TRAP activity of KO cells were suppressed to same extent as Ctrl cells by *Zscan10* overexpression (Fig. 1I).

Total RNA was extracted from cells at Days 0, 2 and 5 after RANKL treatment, and the expression levels of osteoclast differentiation-related genes were examined by RT-qPCR. The expression levels of osteoclast differentiation marker genes, such as *Nfatc1*, *DCstamp*, *Trap* and *Ctsk*, were significantly increased in KO cells (Fig. 2A). On the other hand, the expression level of *Irf8* was significantly decreased among osteoclast differentiation inhibitory factors (Fig. 2B). These results suggested that Zscan10 could negatively regulate osteoclast differentiation through target genes' transcription without affecting cell viability.

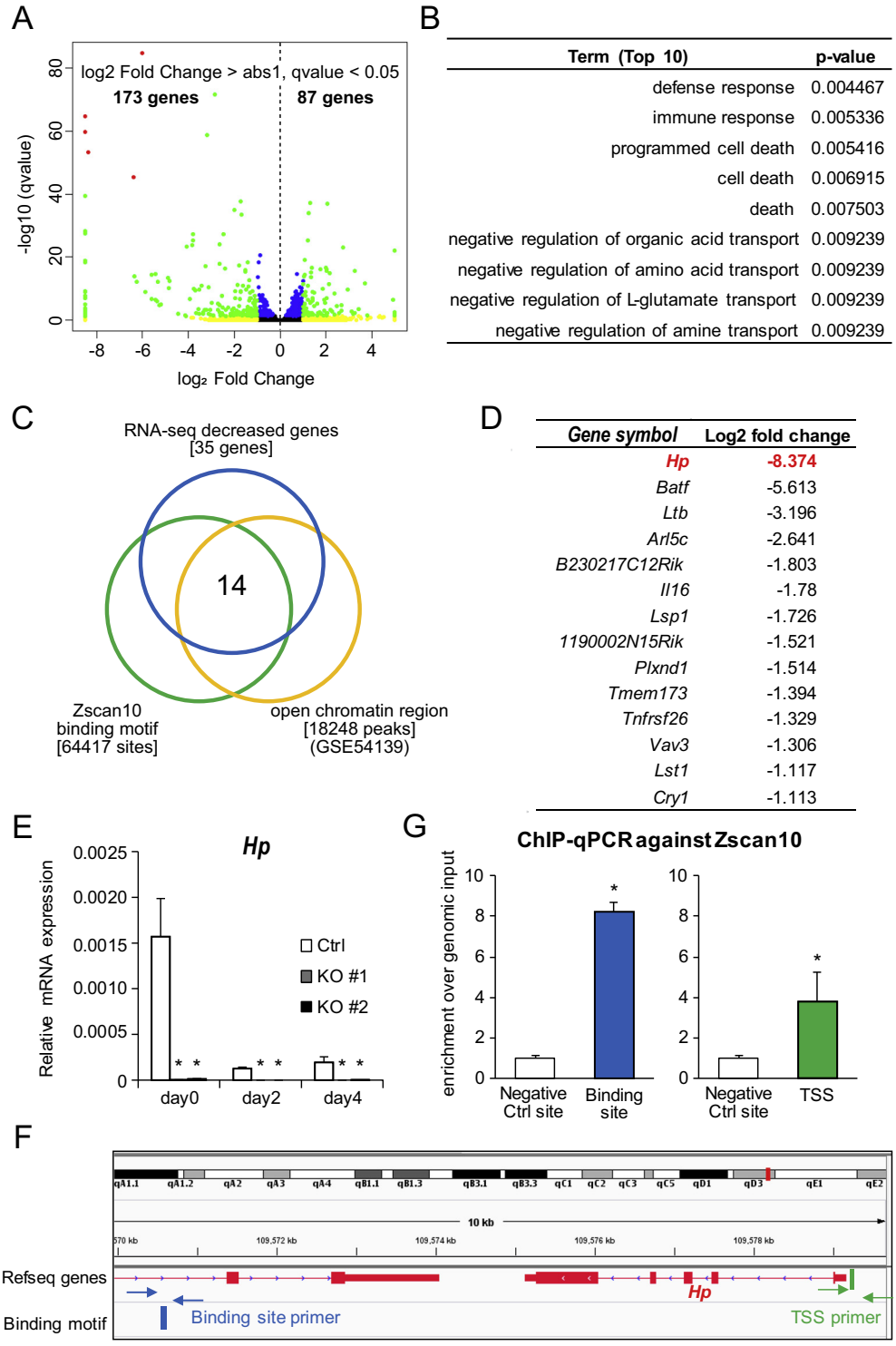

Fig. 3. Identification of genes that could be regulated by Zscan10. (A) Volcano plots of RNA-seq data in KO cells compared with Ctrl cells. (B) Gene Ontology (GO) analyses were performed using DAVID Bioinformatics Resources. GO KEGG pathways in the 147 down-regulated genes are illustrated by gene *p* values. (D) Venn diagram to investigate the genes, which is controlled by Zscan10 using decreased genes in KO cells (blue), genes harboring Zscan10 binding motif within 25 kb of the TSS (green) and open chromatin region (yellow). (E) Validation of *Haptoglobin* (*Hp*) mRNA expression levels associated with osteoclast differentiation by RT-qPCR. (F) Genomic view of the sites for ChIP qPCR. Blue: Zscan10 binding site, Green: *Hp* TSS. (G) ChIP qPCR of the *Hp* gene locus. Enrichment over genomic input using anti-flag antibody. Data represent means ± SD, n = 3. The data were analyzed using a two-tailed Student's *t*-test or a one-way ANOVA followed by Tukey–Kramer method post hoc tests. Asterisk indicates $p < 0.05$ versus control. (For interpretation of the references to colour in this figure legend, the reader is referred to the web version of this article.)

3.2. Immune system genes, including negative regulatory genes for osteoclast differentiation, were reduced by Zscan10 KO

We asked how gene expression was altered by KO of *Zscan10*. Thus, we conducted comprehensive gene expression analysis using RNA-seq for RAW264 cells in the absence of RANKL treatment. We found that in KO cells the expression levels of 173 genes were significantly decreased to < 50% whereas the expression levels of 87 genes were significantly increased by > 2-fold compared with Ctrl cells (Fig. 3A, Supplemental Table S2A and B). Osteoclast differentiation inhibitory factors such as *Cd74* and *Fcgr2b* were included among the 173 downregulated genes, (Supplemental Table S3A). In addition, GO analyses revealed that the biological process of the immune system (Supplemental Table S3A) and tissues of B-cells and the spleen (Supplemental Table S3B) were enriched among the differentially expressed genes by Zscan10 KO (Fig. 3B). These results indicated that Zscan10 may specifically govern transcription of the genes related to immunological responses including differentiation of macrophages and/or macrophage derived osteoclasts.

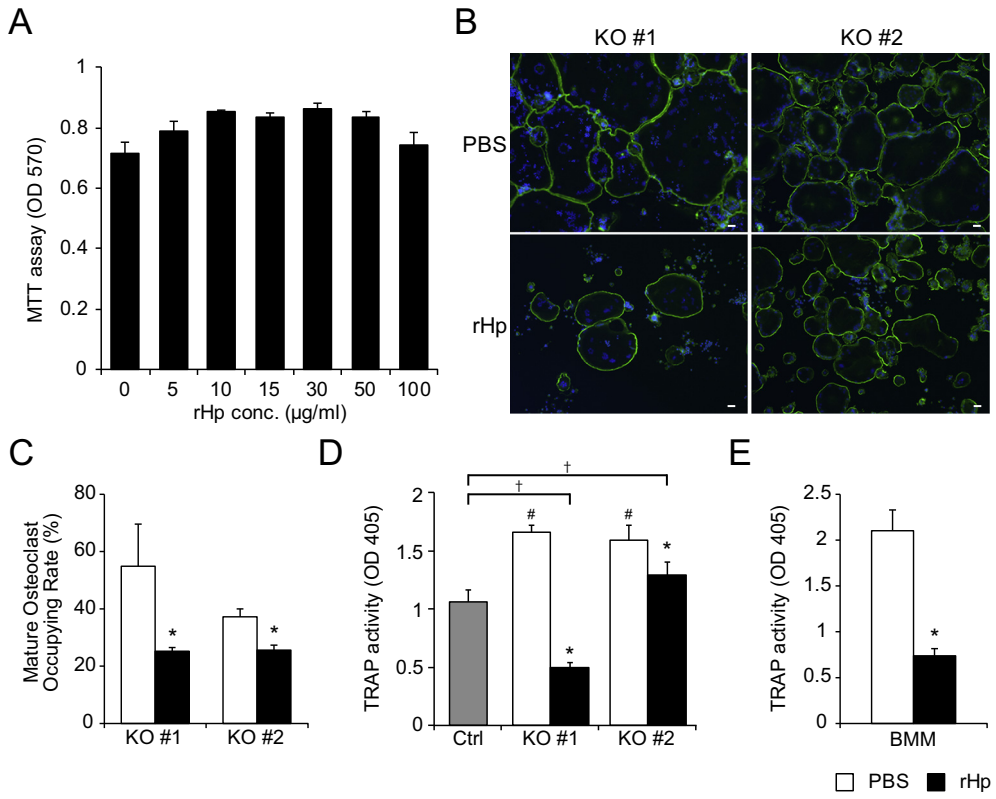

Fig. 4. Recombinant Hp treatment affects osteoclast differentiation. (A) Cell viability assay of rHp-treated RAW264 cells determined by MTT assay. (B) Fluorescence staining of rHp-treated KO cells; nuclear (blue) and actin (green). Bars indicate 50 μm. (C) Percentage of mature osteoclasts occupying arbitrary area. (D) TRAP activity of rHp-treated Ctrl and KO cells. (E) TRAP activity of rHp-treated BMM. Data represent means ± SD, n = 3. The data were analyzed using a two-tailed Student's *t*-test or a one-way ANOVA followed by Tukey–Kramer method as post hoc tests. Asterisk indicates $p < 0.05$ versus PBS. Sharp indicates $p < 0.05$ versus Ctrl. Dagger indicates $p < 0.05$ between groups. (For interpretation of the references to colour in this figure legend, the reader is referred to the web version of this article.)

3.3. *Zscan10* directly controlled the transcription of *Hp*

Next, we identified the genes that were most crucial for osteoclast differentiation among those that were significantly down-regulated by *Zscan10* KO. Thus, we performed stringent analyses using 2 different RNA-seq analyses, such as TMM and FPKM methods. Only 35 genes overlapped in the analyses (Supplemental Fig. S3). To identify direct target genes of Zscan10, we started with those 35 genes and performed integrative analysis using genome-wide information of the Zscan10 binding sequence motif [13] and the open chromatin region of RAW264 cells [10] (Fig. 3C). In that way, we identified 14 genes as overlapped genes (Fig. 3D). The *haptoglobin* gene (*Hp*) was identified as the one that was most significantly reduced in KO cells (Fig. 3D). RT-qPCR for *Hp* validated that the mRNA expression level of *Hp* was remarkably decreased in KO cells in spite of the differentiation stages of osteoclasts (Fig. 3E). Since mRNA expression level of *Hp* decreased according to osteoclast differentiation, it is possible that *Hp* might be negatively regulated by Nfatc1. Therefore, to confirm whether transcription of *Hp* was regulated by Nfatc1, we treated RAW264 cells with calcineurin inhibitor, FK506. As a result, FK506 treatment decreased mRNA expression level of *Nfatc1* but not affected *Hp* expression in RAW264 cells (Supplemental Fig. S4). ChIP-qPCR was performed to confirm that Zscan10 bound to the *Hp* gene locus. ChIP-qPCR against Zscan10 revealed that Zscan10 binding was significantly enriched in the Zscan10 binding motif as well as the TSS when compared to the negative Ctrl site (Fig. 3F, G). These results suggest that Zscan10 directly regulated transcription of *Hp*.

3.4. Haptoglobin inhibited osteoclast differentiation

To examine the effect of Hp during Zscan10-mediated osteoclastogenesis, we first assessed the cytotoxicity of rHp on KO cells. We observed no effect of rHp on cell viability, regardless of concentration (Fig. 4A). Therefore, KO cells were treated with 20 μg/mL of rHp. rHp treatment impaired osteoclast differentiation facilitated by *Zscan10* KO (Fig. 4B). Also, the occupied ratio by mature osteoclasts was significantly suppressed by rHp treatment (Fig. 4C). Furthermore, rHp treatment suppressed TRAP activity in KO cells as well as in primary BMM-derived osteoclasts (Fig. 4D, E). Also, rHp treatment tended to suppress the expression levels of osteoclast differentiation marker genes in BMM-derived osteoclasts (Supplemental Fig. S5). These results indicated that *Hp*, a direct target gene of Zscan10, could significantly suppress osteoclast differentiation and that Zscan10 is a negative regulatory transcription factor for osteoclast differentiation.

4. Discussion

Analysis of chromatin remodeling during osteoclastogenesis using DNase-seq suggested that transcription factor Zscan10 might play a functional role in osteoclast differentiation [10]. However, studies of Zscan10 have mainly focused on ES cells [12,14–17,19] and little is known about its role in other settings. To investigate the roles of Zscan10 in osteoclasts, we generated *Zscan10* KO cells. And, to avoid off target effects of genome editing, we established and analyzed two lines of *Zscan10* KO RAW264 cells. These cells found no difference in cell proliferation or survival rate in KO cells, suggesting that Zscan10 is not involved in cell division, at least in a macrophage-like cell lineage. On the other hand, TRAP activity and the expression levels of differentiation marker genes were increased in KO cells (Figs. 1 and 2). Also, the expression of inhibitory factors of osteoclast differentiation was decreased. Additionally, TRAP activity of KO cells were suppressed as much as Ctrl cells by *Zscan10* overexpression. These results indicated that Zscan10 had a role in the negative regulation of osteoclastogenesis without affecting cell proliferation. This observation of Zscan10 function is consistent with a previous report that claimed that Zscan10 was dispensable for mouse development [18].

However, these results were seemingly inconsistent to the results of our previous study, in which osteoclast differentiation was suppressed by siRNA knockdown [10]. The difference between this and previous study was the utilized methods to inactivate *Zscan10* expression,

temporal siRNA knockdown or CRISPR/Cas9 mediated persistent knockout (KO). Different methodology may cause final different phenotypes of osteoclastogenesis because siRNA could only suppress the expression of *Zscan10* only in the beginning of osteoclastogenesis unlike genome editing KO. In addition, RNA-seq for *Zscan10* KO RAW cells showed possible reasons for phenomenon promoting osteoclast differentiation, suggesting that inactivation of *Zscan10* during entire osteoclastogenesis can facilitate osteoclast differentiation.

The genome-wide gene expression analyses using RNA-seq followed by GO analysis of differentially expressed genes revealed that the number of genes with decreased expression in *Zscan10* KO cells was enriched in B-cells and splenic tissues and the biological process of the immune system (Fig. 3). Osteoclasts are well known to be differentiated from monocyte/macrophage cells involved in immunity [29]. RANKL, which is the most important molecule in osteoclast differentiation, was first identified as a dendritic cell activating factor expressed on T cells [30,31]. The concept that key factors in the immune system have important roles in bone metabolism is termed osteoimmunology [32]. Based on that concept, Zscan10 is identified as a novel factor in osteoclastogenesis that might have a functional role in the immune system. Therefore, the clarification of Zscan10 function in the immune system and component cells should be explored. Bioinformatic integrated genome-wide analyses, followed by validation experiments successfully identified possible target genes of Zscan10. Among them, *haptoglobin* (*Hp*) was identified as a target gene of Zscan10. In order to ascertain whether Zscan10 directly or indirectly regulates transcription of *Hp*, we performed calcineurin inhibitor assay and ChIP-qPCR against Zscan10. These results suggested that Zscan10 may directly regulate transcription of *Hp*. ChIP-qPCR confirmed that Zscan10 could bind to the *Hp* gene enhancer region harboring the Zscan10 binding motif as well as the TSS without known consensus sequences (Fig. 3). Zscan10 is a transcription factor that can organize the transcription of genes by the formation of the topology associating domain (TAD) [33]. Stat3 reportedly regulates *Hp* gene expression by binding to the TSS [34]. These data and reports suggest that a transcriptional complex including Zscan10 and Stat3 may coordinately regulate transcription of *Hp*, although chromosome conformation capture analysis should be done to support this idea.

Hp is one of the major acute phase proteins, and its concentration in the circulating blood increases 2–4 fold in several pathologic conditions, such as trauma, cancer and pregnancy [35]. Hp binds strongly to extravascular hemoglobin (Hb) and rapidly removes the toxic Hb via the CD163 scavenger receptor of macrophages [36]. It was reported that osteoclasts were activated by Hp. [37] On the other hand, *Hp* KO mice exhibit decreased bone mass and increased osteoclast number, and Hp has been reported to be involved in suppression of osteoclast differentiation [38]. The role of Hp in osteoclast-mediated bone metabolism remains controversial. In this study, we found that rHp treatment significantly suppressed osteoclast differentiation in *Zscan10* KO RAW264 cells as well as BMMs. Whereas these data suggest that Hp works on osteoclasts in an autocrine or paracrine manner, Hp is mainly produced in the liver. This point should be further studied. Patients with hemolytic disease are known to have lower levels of Hp in the blood [39]. Furthermore, low bone mineral density and fractures are frequent in patients suffering from hemolytic hemoglobinopathies [40] and there is a report that hemolytic mice exhibit decreased bone mineral density [41], indicating that Hp has protective effects for bone metabolism even *in vivo*. The limitation of this study is that we could not examine *Zscan10* and *Hp* KO mouse phenotypes to display physiological function of Zscan10. These studies should be done as the future study. However, our study revealed that Zscan10, which has been identified as a novel transcription factor candidate in osteoclast differentiation, negatively regulates osteoclast differentiation through direct regulation of *Hp* transcription. We also showed that Hp can negatively regulate osteoclasts and has protective effects on bone metabolism.

Supplementary data to this article can be found online at https://doi.org/10.1016/j.bone.2019.02.011.

Disclosure statement

All authors state that they have no conflicts of interest.

Acknowledgments

The authors thank Dr. Naohito Tokunaga, staff of the Division of Analytical Bio-Medicine and the Division of Laboratory Animal Research, Advanced Research Support Center (ADRES), Ms. Aya Tamai and Ms. Sayoko Nakanishi of the Division of Integrative Pathophysiology, Proteo-Science Center (PROS), Ehime University for their technical assistance and helpful support. This study was supported in part by JSPS KAKENHI Grants (17K19728), Japan Osteoporosis Foundation and Mitsui Life Social Welfare Foundation to YI.

Authors' roles

YY, KI and YI planned the study and designed the experiments. NS, YS and SY assisted with design of experiments and interpretation of the data. JWL and TI performed histological examinations and assisted with interpretation of the data. YY and YI wrote the manuscript, with input from the other authors.

References

[1] T.J. Martin, N.A. Sims, Osteoclast-derived activity in the coupling of bone formation to resorption, Trends Mol. Med. 11 (2) (Feb 2005) 76–81 (Epub 2005/02/08).
[2] S.L. Teitelbaum, Bone resorption by osteoclasts, Science (New York, N.Y.) 289 (5484) (Sep 1 2000) 1504–1508 (Epub 2000/09/01).
[3] S.L. Teitelbaum, F.P. Ross, Genetic regulation of osteoclast development and function, Nat. Rev. Genet. 4 (2003) 638 Review Article 08/01/online.
[4] H. Takayanagi, S. Kim, T. Koga, H. Nishina, M. Isshiki, H. Yoshida, et al., Induction and activation of the transcription factor NFATc1 (NFAT2) integrate RANKL signaling in terminal differentiation of osteoclasts, Dev. Cell 3 (6) (2002) 889–901 2002/12/01/.
[5] T. Yamashita, Z. Yao, F. Li, Q. Zhang, I.R. Badell, E.M. Schwarz, et al., NF-kappaB p50 and p52 regulate receptor activator of NF-kappaB ligand (RANKL) and tumor necrosis factor-induced osteoclast precursor differentiation by activating c-Fos and NFATc1, J. Biol. Chem. 282 (25) (Jun 22 2007) 18245–18253 (Epub 2007/05/09).
[6] E.F. Wagner, R. Eferl, Fos/AP-1 proteins in bone and the immune system, Immunol. Rev. 208 (Dec 2005) 126–140 (Epub 2005/11/30).
[7] K. Sato, A. Suematsu, T. Nakashima, S. Takemoto-Kimura, K. Aoki, Y. Morishita, et al., Regulation of osteoclast differentiation and function by the CaMK-CREB pathway, Nat. Med. 12 (2006) 1410 11/26/online.
[8] C.P. Price, A. Kirwan, C. Vader, Tartrate-resistant acid phosphatase as a marker of bone resorption, Clin. Chem. 41 (5) (May 1995) 641–643 (Epub 1995/05/01).
[9] F.H. Drake, R.A. Dodds, I.E. James, J.R. Connor, C. Debouck, S. Richardson, et al., Cathepsin K, but not cathepsins B, L, or S, is abundantly expressed in human osteoclasts, J. Biol. Chem. 271 (21) (May 24 1996) 12511–12516 (Epub 1996/05/24).
[10] K. Inoue, Y. Imai, Identification of novel transcription factors in osteoclast differentiation using genome-wide analysis of open chromatin determined by DNase-seq, J. Bone Miner. Res. 29 (8) (Aug 2014) 1823–1832.
[11] K. Inoue, Y. Imai, Fatostatin, an SREBP inhibitor, prevented RANKL-induced bone loss by suppression of osteoclast differentiation, Biochim. Biophys. Acta 1852 (11) (Nov 2015) 2432–2441 (Epub 2015/09/01).
[12] Z.X. Wang, J.L. Kueh, C.H. Teh, M. Rossbach, L. Lim, P. Li, et al., Zfp206 is a transcription factor that controls pluripotency of embryonic stem cells, Stem Cells 25 (9) (Sep 2007) 2173–2182 (Epub 2007/07/12).
[13] H.B. Yu, G. Kunarso, F.H. Hong, L.W. Stanton, Zfp206, Oct4, and Sox2 are integrated components of a transcriptional regulatory network in embryonic stem cells, J. Biol. Chem. 284 (45) (Nov 2009) 31327–31335 (Epub 2009/09/09).
[14] Z.X. Wang, C.H. Teh, J.L. Kueh, T. Lufkin, P. Robson, L.W. Stanton, Oct4 and Sox2 directly regulate expression of another pluripotency transcription factor, Zfp206, in embryonic stem cells, J. Biol. Chem. 282 (17) (Apr 27 2007) 12822–12830 (Epub 2007/03/09).
[15] W. Zhang, E. Walker, O.J. Tamplin, J. Rossant, W.L. Stanford, T.R. Hughes, Zfp206 regulates ES cell gene expression and differentiation, Nucleic Acids Res. 34 (17) (2006) 4780–4790 (Epub 2006/09/13).
[16] M. Skamagki, C. Correia, P. Yeung, T. Baslan, S. Beck, C. Zhang, et al., ZSCAN10 expression corrects the genomic instability of iPSCs from aged donors, Nat. Cell Biol. 19 (9) (Sep 2017) 1037–1048 (Epub 2017/08/28).
[17] D. Papatsenko, H. Darr, I.V. Kulakovskiy, A. Waghray, V.J. Makeev, B.D. MacArthur, et al., Single-cell analyses of ESCs reveal alternative pluripotent cell states and molecular mechanisms that control self-renewal, Stem Cell Rep. 5 (2)

(Aug 2015) 207–220.
[18] P. Kraus, S. V, H.B. Yu, X. Xing, S.L. Lim, T. Adler, et al., Pleiotropic functions for transcription factor zscan10, PLoS One 9 (8) (2014) e104568(Epub 2014/08/11).
[19] M. Yamane, S. Fujii, S. Ohtsuka, H. Niwa, Zscan10 is dispensable for maintenance of pluripotency in mouse embryonic stem cells, Biochem. Biophys. Res. Commun. 468 (4) (Dec 2015) 826–831 (Epub 2015/11/22).
[20] T.G. Montague, J.M. Cruz, J.A. Gagnon, G.M. Church, E. Valen, CHOPCHOP: a CRISPR/Cas9 and TALEN web tool for genome editing, Nucleic Acids Res. 42 (W1) (2014) W401–W407.
[21] K. Labun, T.G. Montague, J.A. Gagnon, S.B. Thyme, E. Valen, CHOPCHOP v2: a web tool for the next generation of CRISPR genome engineering, Nucleic Acids Res. 44 (W1) (2016) W272–W276.
[22] J.W. Lee, A. Hoshino, K. Inoue, T. Saitou, S. Uehara, Y. Kobayashi, et al., The HIV co-receptor CCR5 regulates osteoclast function, Nat. Commun. 8 (1) (Dec 2017) 2226 (Epub 2017/12/20).
[23] W.S. Rasband, ImageJ, U S National Institutes of Health, Bethesda, Maryland, USA, 1997-2018.
[24] D.W. Huang, B.T. Sherman, R.A. Lempicki, Systematic and integrative analysis of large gene lists using DAVID bioinformatics resources, Nat. Protoc. 4 (2008) 44 12/18/online.
[25] da W. Huang, B.T. Sherman, R.A. Lempicki, Bioinformatics enrichment tools: paths toward the comprehensive functional analysis of large gene lists, Nucleic Acids Res. 37 (1) (Jan 2009) 1–13 (Epub 2008/11/27).
[26] E. Afgan, D. Baker, B. Batut, M. van den Beek, D. Bouvier, M. Cech, et al., The Galaxy platform for accessible, reproducible and collaborative biomedical analyses: 2018 update, Nucleic Acids Res. 46 (W1) (Jul 2 2018) W537–W544 (Epub 2018/05/24).
[27] J.T. Robinson, H. Thorvaldsdottir, W. Winckler, M. Guttman, E.S. Lander, G. Getz, et al., Integrative genomics viewer, Nat. Biotechnol. 29 (1) (Jan 2011) 24–26 (Epub 2011/01/12).
[28] H. Thorvaldsdottir, J.T. Robinson, J.P. Mesirov, Integrative Genomics Viewer (IGV): high-performance genomics data visualization and exploration, Brief. Bioinform. 14 (2) (Mar 2013) 178–192 (Epub 2012/04/21).
[29] H. Takayanagi, Osteoimmunology: shared mechanisms and crosstalk between the immune and bone systems, Nat. Rev. Immunol. 7 (2007) 292 Review Article 04/01/online.
[30] D.M. Anderson, E. Maraskovsky, W.L. Billingsley, W.C. Dougall, M.E. Tometsko, E.R. Roux, et al., A homologue of the TNF receptor and its ligand enhance T-cell growth and dendritic-cell function, Nature 390 (1997) 175 11/13/online.
[31] B.R. Wong, J. Rho, J. Arron, E. Robinson, J. Orlinick, M. Chao, et al., TRANCE is a novel ligand of the tumor necrosis factor receptor family that activates c-Jun N-terminal kinase in T cells, J. Biol. Chem. 272 (40) (Oct 3 1997) 25190–25194 (Epub 1997/10/06).
[32] K. Okamoto, T. Nakashima, M. Shinohara, T. Negishi-Koga, N. Komatsu, A. Terashima, et al., Osteoimmunology: the conceptual framework unifying the immune and skeletal systems, 97 (4) (2017) 1295–1349.
[33] S. Aranda, G. Mas, L. Di Croce, Regulation of gene transcription by Polycomb proteins, Sci. Adv. 1 (11) (Dec 2015) e1500737(Epub 2015/12/15).
[34] H. Kim, H. Baumann, The carboxyl-terminal region of STAT3 controls gene induction by the mouse haptoglobin promoter, J. Biol. Chem. 272 (23) (Jun 6 1997) 14571–14579 (Epub 1997/06/06).
[35] H. Baumann, J. Gauldie, The acute phase response, Immunol. Today 15 (2) (Feb 1994) 74–80 (Epub 1994/02/01).
[36] M.J. Nielsen, S.K. Moestrup, Receptor targeting of hemoglobin mediated by the haptoglobins: roles beyond heme scavenging, Blood 114 (4) (Jul 23 2009) 764–771 (Epub 2009/04/22).
[37] U.H. Lerner, N. Frohlander, Haptoglobin-stimulated bone resorption in neonatal mouse calvarial bones in vitro, Arthritis Rheum. 35 (5) (May 1992) 587–591 (Epub 1992/05/01).
[38] Z.H. Lee, H.H. Kim, J.O. Kwon, Haptoglobin acts as a novel ligand for TLR4, suppressing osteoclastogenesis via activation of TLR4 - INF-β signaling pathway, ASBMR 2018 Annual Meeting.MON-0644, 2018.
[39] W. Barcellini, B. Fattizzo, Clinical applications of hemolytic markers in the differential diagnosis and management of hemolytic anemia, Dis. Markers 2015 (2015) 635670 (Epub 2015/12/27).
[40] T.D. Faber, D.C. Yoon, S.C. White, Fourier analysis reveals increased trabecular spacing in sickle cell anemia, J. Dent. Res. 81 (3) (Mar 2002) 214–218 (Epub 2002/03/06).
[41] R. Moreau, D. Tshikudi Malu, M. Dumais, E. Dalko, V. Gaudreault, H. Roméro, et al., Alterations in bone and erythropoiesis in hemolytic anemia: comparative study in bled, phenylhydrazine-treated and plasmodium-infected mice, PLoS One 7 (9) (2012) e46101(Epub 2012/09/28).